Water Tetrahedrons, Hydrogen-Bond Dynamics, and the Orientational Mobility of Water around Hydrophobic Solutes

ARTICLE *in* THE JOURNAL OF PHYSICAL CHEMISTRY B · MARCH 2014

Impact Factor: 3.3 · DOI: 10.1021/jp500067a · Source: PubMed

1 AUTHOR:

Nuno Galamba

24 PUBLICATIONS **311** CITATIONS

SEE PROFILE

THE JOURNAL OF PHYSICAL CHEMISTRY B

Article

pubs.acs.org/JPCB

Water Tetrahedrons, Hydrogen-Bond Dynamics, and the Orientational Mobility of Water around Hydrophobic Solutes

N. Galamba*

Grupo de Física-Matemática da Universidade de Lisboa, Av. Prof. Gama Pinto 2, 1649-003 Lisboa, Portugal

Supporting Information

ABSTRACT: Despite being intensively studied, the magnitude of specific structural and dynamic perturbations of water next to hydrophobic surfaces remains a matter of debate. Here we show, from molecular dynamics, that the structure of a subset of water molecules in the first hydration layer, those preserving four nearest water neighbors, resembles that of water at ∼10 °C, and that the origin of the orientational slowdown is mainly a decrease of the hydrogen-bond (HB) acceptor switch frequency, while water structuring plays a minor role, slightly accelerating HB acceptor switches. By portraying the mean HB dynamics of water as a doubly periodic event, we demonstrate that the orientational retardation factor is effectively defined by the ratio of the HB acceptor switch period in the hydration layer and bulk. Excluded volume delays HB acceptor switches, accelerating the orientational relaxation of ∼1/3 of the water molecules on the hydration layer in this time scale, but this is largely exceeded by the decrease of the HB switch frequency, consistent with 2D IR spectroscopy experiments, and at the origin of longer HB lifetimes. The orientational mobility of water populations with long HB lifetimes is also probed, and although a relaxation plateau is observed at ∼10 ps consistent with fs IR spectroscopy experiments, no water molecule is rotationally frozen at any time scale. The proposed molecular picture is consistent with fs IR, 2D IR, and NMR experimental results on the orientational retardation of water and reveals the magnitude of "hidden" enhanced ordered water pentamers formed near hydrophobic solutes.

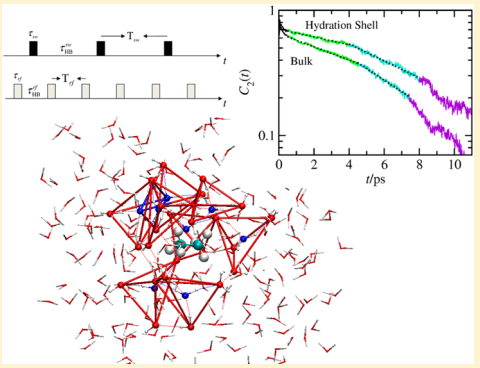

INTRODUCTION

Hydrophobic hydration and interactions play key roles in many chemical and biological processes such as micelle formation, protein folding, or membrane self-assembly.[1−4] The hydration of apolar solutes at room temperature is characterized by a large decrease of the entropy and an increase of the heat capacity of solution. Frank and Evans[5] proposed in 1945 the so-called "iceberg" model to explain the thermodynamics of hydrophobic hydration, according to which water molecules in the vicinity of apolar groups adopt a more "crystalline" structure.[3,5,6] Even though the "iceberg" model provides a plausible explanation of the thermodynamics of hydrophobic hydration at room temperature, direct experimental evidence of enhanced water structuring around hydrophobic molecules has never been found.[7−9] This further precluded support to the entropic origin of hydrophobic interactions proposed by Kauzmann[1,3] in 1959, which rested on the existence of an entropic attractive force between hydrophobic groups, whose origin was the release (to the bulk) of water molecules forming "ice-like" structures around hydrophobic groups, resulting in the increase of entropy. Thus, alternative models and theories have been proposed to explain the thermodynamics of hydrophobic hydration[2,6,10−17] that do not resort to water structuring assertions. Nevertheless, and even though it is widely accepted that no literal ice-like water structures form, water's reorganization around hydrophobic solutes remains unclear, namely, whether water is more/less structured or similar to bulk water. On a recent molecular dynamics (MD) study,[18] a significant tetrahedrality enhancement on a subset of water molecules in the first hydration layer of small apolar solutes was found, thus bearing some resemblances with a moderate view of the "iceberg" model. A similar enhancement was also recently reported near methane from MD of a coarse grained water model.[19] A tetrahedrality enhancement of water had also been previously reported in minor grooves of DNA[20] from MD and in the first hydration shell of alcohols from Raman scattering experiments.[21]

Hydrophobic hydration is also characterized by a slowdown[22−34] of the orientational (and translational) dynamics of water near apolar groups. This slowdown has been associated with both stronger HBs and excluded volume water depletion, but the significance of the above-mentioned tetrahedrality enhancement and excluded volume effects remain to be fully understood. Further, the extent of this orientational retardation is controversial with femtosecond mid-infrared (fs IR) spectroscopy results indicating that two to four water molecules (four OH groups) on average are effectively immobilized around methyl groups on a 10 ps time scale.[31] This strong

Received: January 3, 2014
Revised: March 19, 2014
Published: March 24, 2014

   dx.doi.org/10.1021/jp500067a | J. Phys. Chem. B 2014, 118, 4169−4176

slowdown has been further supported by 2D IR spectroscopy[24] results but is in conflict with MD,[35−44] NMR,[22,23,26,27,29,30,32,34] and dielectric relaxation spectroscopy,[28,33] which foresee a mild slowdown of the orientational dynamics of water next to hydrophobic groups. A slow rotational time in the hydration shell of tetramethylurea, consistent with that from fs IR spectroscopy,[31] was also found in a recent Car−Parrinello MD study.[45] Other CPMD works, nonetheless, on the hydration of methane[40] and methanol[42] indicated a moderate slowdown in line with classical MD. The existence of immobilized water molecules in the vicinity of hydrophobic groups hints at the possibility that some water molecules have exceedingly long HB lifetimes. Here we probe the orientational mobility and HB dynamics of water molecules in the hydration layer of four archetypal small hydrophobic solutes, in particular, xenon, methane, ethane, and benzene. We then proceed to investigate the orientational dynamics of specific subsets of water molecules with long HB lifetimes. The tetrahedrality of water is calculated in the vicinity of the solutes, and we compare both the structure and dynamics of water with those of neat water at low temperatures. The relationship between the structural transformations and the orientational dynamics of water next to the hydrophobic solutes is then discussed.

METHODS

Molecular dynamics (MD) simulations of a single atom of Xe, or of a single molecule of CH_4, C_2H_6, and C_6H_6, and 256 water molecules, at 298.15 K and 1 atm, were carried out in the (N, V, E) ensemble, with the flexible and polarizable force field AMOEBA 04;[46,47] the MD were performed with the program Tinker.[48] Electrostatic interactions were calculated with the Ewald sum. The MD were carried out for 3.0 ns, with a modified Beeman algorithm and a time step of 0.5 fs after more than 1 ns in the (N, P, T) environment[49] for equilibration purposes. The average temperatures for the Xe, CH_4, C_2H_6, and C_6H_6 solutions were, respectively, 297, 301, 300, and 298 K. MD for pure water at 298.15 and 283.15 K and 1 atm were also performed in the (N, P, T) ensemble with a Nosé−Hoover thermostat and barostat for comparison purposes (see the Supporting Information). HBs were defined by the following geometric criteria: $r_{OO} < 3.5$ Å and $\phi_{HOO} < 30°$, where r_{OO} is the distance between the donor and acceptor oxygen atoms and ϕ_{HOO} is the angle between the intramolecular O−H bond and r_{OO}. HB lifetime probability distribution functions[50−52] for water were calculated from $p(t) = N_{HB}(t, \Delta t)/\sum_t N_{HB}(t, \Delta t)$, where $N_{HB}(t, \Delta t)$ is the number of donor (or acceptor) HBs that (i) remained unbroken at all times up to $t \pm \Delta t/2$ and (ii) got broken at $t \pm \Delta t/2$. $N_{HB}(t, \Delta t)$ was calculated through sampling of every time origin, Δt was set to 2.5 fs, and the mean (continuous) HB lifetime (or mean first passage time[53]) was obtained from $\tau_{HB} = \int_0^\infty tP(t)\,dt$. The passage across the solutes' hydration shell of water molecules with unbroken HBs was accounted for through a protocol previously described[51] (see the Supporting Information). The HB lifetimes of pure water, in the region corresponding to the first and second self-hydration shells (see the Supporting Information for details) were also probed for comparison purposes; a single water molecule was defined as the solute and HBs between water molecules in the self-hydration shell and the "solute" water molecules were neglected.

RESULTS AND DISCUSSION

Orientational and Hydrogen-Bond Dynamics. The orientational mobility of water was probed through the calculation of the orientational autocorrelation function, $C_2(t) = P_2[\mathbf{u}_{r_{OH}}(t)\cdot\mathbf{u}_{r_{OH}}(t + dt)]$, where $\mathbf{u}_{r_{OH}}$ is the intramolecular OH unit vector and P_2 is the second-order Legendre polynomial (Figure 1). The orientational times, τ, obtained from the time

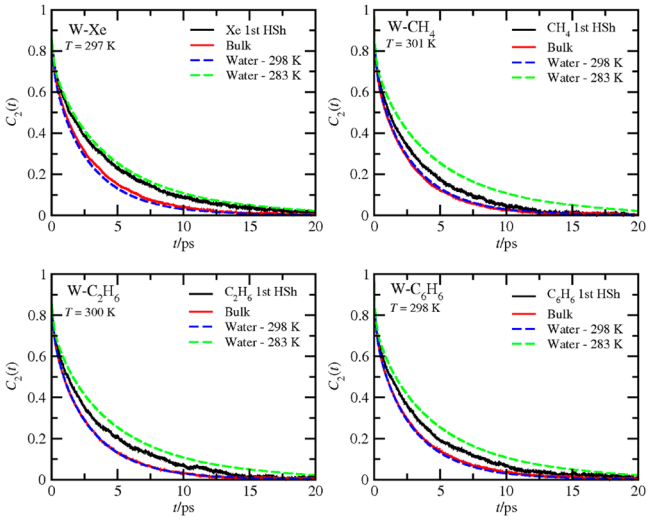

Figure 1. Orientational autocorrelation functions for water molecules initially in the first hydration shell and bulk for the distinct solutions and for neat water (full system) at 298 and 283 K; the bulk is considered the region beyond the second hydration layer of the solutes.

Table 1. Orientational Times, τ, for the First Hydration Shell (HSh) and Bulk for the Different Solutes

	τ (ps) 1st HSh	τ (ps) bulk	τ_{HSh}/τ_{bulk}
$(H_2O)_{298K}$		2.2[a]	
$(H_2O)_{283K}$		3.7[a]	
$(Xe)_{aq,297K}$	3.3	2.4	1.4[b]
$(CH_4)_{aq,301K}$	2.6	2.0	1.3
$(C_2H_6)_{aq,300K}$	2.9	2.1	1.4
$(C_6H_6)_{aq,298K}$	2.9	2.2	1.3[c]

[a]Orientational times for the full system; NMR relaxation times for water at 298 K are in the range 1.7−2.6 ps.[54] [b]NMR[26] τ_{HSh}/τ_{bulk} for Xe−D_2O is 1.3 at 298 K for a (MD) coordination number $N_h = 21.5$ similar to the $N_h = 21.4$ found here. [c]NMR[23] τ_{HSh}/τ_{bulk} for C_6H_6−D_2O is 1.5 at 303 K for a (MD) $N_h = 23$ smaller than the $N_h = 29.1$ found here; for $N_h = 29.1$, a retardation factor of 1.4 is obtained.

integral of $C_2(t)$ for the distinct solutions are given in Table 1. A moderate slowdown, by a factor of less than 2, of the orientational mobility of water in the solutes' hydration shell can be observed, in good accord with NMR and MD studies of distinct hydrophobic solutes. Further, it can be seen that the orientational dynamics is slower and faster, respectively, than for pure water at 298 and 283 K. These $C_2(t)$ functions have, nevertheless, a contribution from water molecules that crossed the hydration shell (or the bulk) during the 20 ps time scale considered (see the Supporting Information). In addition, a subset of water molecules in the hydration layer, those in direct

dx.doi.org/10.1021/jp500067a | J. Phys. Chem. B 2014, 118, 4169−4176

interaction with the solute, should have a distinctive mobility from those further away, where excluded volume effects are less important.

Hence, to gain further insight on the magnitude and origin of the orientational slowdown, we computed HB lifetime probability distributions and probed the orientational mobility of specific subsets of water molecules in the solutes' hydration shell. The mean HB lifetimes, τ_{HB}, in the solutes' hydration shell are longer than for bulk and neat water at room T and lower than for water at 283 K, consistent with the orientational slowdown of water (see Table 2).

Table 2. HB Donor Continuous Lifetimes, τ_{HB}, for the First Hydration Shell (HSh) and Bulk for the Distinct Solutes and Neat Water[a]

	τ_{HB} (ps)		
	1st HSh[b]	bulk[c]	$\tau_{HB}^{HSh}/\tau_{HB}^{bulk}$
$(H_2O)_{298K}$	0.18	0.19	
$(H_2O)_{283K}$	0.22	0.23	
$(Xe)_{aq,297K}$	0.22	0.19	1.2
$(CH_4)_{aq,301K}$	0.20	0.19	1.1
$(C_2H_6)_{aq,300K}$	0.21	0.19	1.1
$(C_6H_6)_{aq,298K}$	0.20	0.19	1.1

[a]For pure water, a single water molecule was taken as the solute and HBs between water molecules in the self-hydration shell and the "solute" water molecule were neglected. [b]For pure water, τ_{HB} was computed for water molecules in the first and second self-hydration shells (see Methods); HB lifetimes of water at 298 and 283 K in the first self-hydration shell are 0.16 and 0.20 ps, respectively. [c]The bulk region for neat water was defined as the region beyond the second self-hydration shell, similar to the aqueous solution definition; HB lifetimes of water at 298 and 283 K for the full systems are equal to the bulk values.

The ratio, $\tau_{HB}^{Hsh}/\tau_{HB}^{bulk}$, is, however, much lower than τ_{HSh}/τ_{bulk}, indicating that the orientational retardation of water is not determined by the (continuous) τ_{HB}; it is shown below that instead of τ_{HB} the orientational slowdown is mostly defined by the HB break/form "period", while τ_{HB} is determined by the HB break/reform dynamics, not significantly perturbed near the hydrophobic solutes. First, however, we address the magnitude of the orientational retardation of water next to the hydrophobic solutes. We calculated $C_2(t)$ for water populations in the first hydration shell and in the bulk, with τ_{HB} longer than some threshold time (here we report results for $\tau_{HB} \geq 4$ ps); the mean number of OH groups with $\tau_{HB} \geq 4$ ps per 10 ps time interval found in the solutes' hydration layer was ~1.0 and ~0.6 for C_2H_6 and CH_4, respectively, and ~1.3 for both Xe and C_6H_6. $C_2(t)$ for these subsets are shown in Figure 2 for methane and ethane (semilog plots for the four solutes are given in the Supporting Information, Figure S1). An ~4 ps exponential region can be seen, where orientational relaxation is very slow, followed by increasingly faster relaxation regions associated with the breakdown of HBs, with the possible crossing of some water molecules outside the hydration shell. Note that beyond the 4 ps time window different HB break/(re)form events occur, including HBs that remain intact, HBs that switch acceptors, and HBs that break and reform with the original acceptor after some transient time; because the probed water subset is small, this leads to the different relaxation regimes observed in Figure 2. Further, despite similar subsets existing in bulk water, the orientational relaxation is faster; the

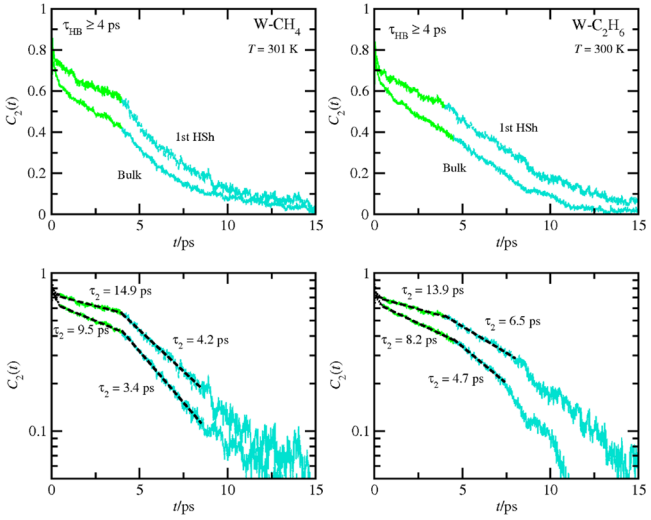

Figure 2. Orientational autocorrelation functions for water molecules with at least one unbroken HB for a minimum of 4.0 ps in the first hydration shell and bulk for the methane and ethane aqueous solutions. $C_2(t)$ were calculated for both OH groups of every water molecule sampled. The orientational relaxation times, τ_2, from monoexponential fits are shown.

reason is, as discussed below, that the second OH group has a lower HB break/form period and therefore a larger orientational mobility in bulk water. A small flat region can also be observed around 10 ps, especially for ethane, which could indicate immobilization of this subset of water molecules (OH groups) on a ~10 ps time scale;[31] it should be stressed that $C_2(t)$ values in Figure 2 are not directly comparable to fs IR experiments, since we consider only a small subset of water molecules in the first hydration layer; these waters are expected to be, however, the slowest waters near the solute and should therefore be at the origin of any long-time residual anisotropy observed experimentally near CH_3 groups.

Large fluctuations occur, nevertheless, at long times, and more importantly this plateau appears both for water in the hydration shell and in the bulk followed by a strong decorrelation beyond the experimentally accessible 10 ps time scale. Thus, despite a plateau apparently similar to that reported from fs IR,[31] indicating a large residual anisotropy ($2/5C_2(t)$) at long delay times, can be observed, no water molecule is, in our view, immobilized at any time scale. Water populations with longer (intermittent) HB lifetimes can be found if transiently (~0.1 ps) broken HBs are neglected; $C_2(t)$ decays faster for these water ensembles for $t \leq \tau_{HB}$ due to librational motions, and slower for $t > \tau_{HB}$, but no evidence of immobilization is found (see the Supporting Information, Figure S2).

We consider now the origin of the longer HB lifetimes and the related[35,38] orientational slowdown in the solutes' hydration shell. Water molecules can form two acceptor and two donor HBs, establishing a random network with a local (approximately) tetrahedral orientational order. When a HB (donor) breaks, it can either reform with the same acceptor after some (transient) *reform time* or switch acceptors after some *switch time*. The switch time can actually be zero if a bifurcated "transition state" is approached where the donor binds to a new acceptor before it breaks with the old one.[55−58] This transition state was observed on a MD study for ~60% of the observed switches, and the water reorientation mechanism was shown to proceed through large amplitude (~60°) angular jumps.[56] This

dx.doi.org/10.1021/jp500067a | J. Phys. Chem. B 2014, 118, 4169−4176

mechanism was also identified near hydrophobic groups, and a mild orientational slowdown of water was associated with a slower jump time, from a stable HB to another,[39] described by a solute excluded volume effect in the reorientation mechanism.[39] Here, we probed the probability of a broken HB to switch acceptors or reform with the original acceptor after a time t and the respective switch and reform mean times. These probability functions were defined by

$$P_{sw}(t) = N_{sw}(t, \Delta t)/\sum_t N_{sw}(t, \Delta t),$$
$$P_{rf}(t) = N_{rf}(t, \Delta t)/\sum_t N_{rf}(t, \Delta t) \quad (1)$$

and the respective, (mean) switch and reform times,

$$\tau_{sw} = \int_0^\infty tP_{sw}(t)\,dt, \qquad \tau_{rf} = \int_0^\infty tP_{rf}(t)\,dt \quad (2)$$

where $N_{sw}(t, \Delta t)$ and $N_{rf}(t, \Delta t)$ are, respectively, the number of broken HBs that switch acceptors and reform with the original acceptor at time $t \pm \Delta t$, after the HB broke. Further, the frequencies, f, of HB break/form (*switch*) and HB break/reform (*reform*) were calculated, that is, the mean number of HBs that break/form or break/reform per unit of time and water molecule; broken HBs that cross the hydration shell (or the bulk) before they either switch acceptors or reform with the original acceptor were neglected. Figure 3 shows the probability

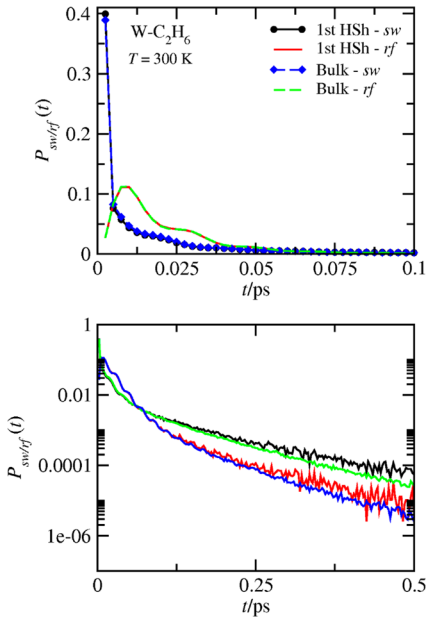

Figure 3. Probability distribution functions $P_{sw}(t)$ and $P_{rf}(t)$ for the first hydration shell and bulk for the ethane aqueous solution. $P_{sw}(t)$ and $P_{rf}(t)$ give, respectively, the probability of a HB donor to switch acceptors and to reform with the original acceptor, t picoseconds after the HB broke. The probability of a HB donor to switch acceptors after 0 ps is shifted to the first positive bin and corresponds to ~30%.

of a broken HB to switch acceptors or reform with the original acceptor at time t, for the ethane solution; similar distributions were obtained for neat water and for the other solutes.

We find that both for neat water and for the hydration shell of the distinct solutes and bulk, 30−35% of the broken HBs switch acceptors after t_{sw} = 0 ps, that is, through a bifurcated "transition state"; notice this refers to every switch event and not only to HB acceptor switches leading to stable new HBs. On the other hand, ~92% of the HBs break and form in less than 0.1 ps and ~98% break and reform in the same time scale (the time scale of librations); these times are consistent with 2D IR and MD calculations that indicate that virtually all water molecules return to a HB partner in 0.2 ps.[59]

From Table 3, it can be seen that the switch time of water molecules in the solutes' hydration layer is longer than that in the bulk and the longest switch time, except for the "solute" water, is observed next to benzene, consistent with its ability to form HO−H···π HBs,[60−64] stronger than aliphatic hydrocarbon−water interactions. Thus, because water−solute interactions are much weaker than water−water interactions, water molecules with a broken HB next to a hydrophobic solute should have enhanced orientational mobility, relative to bulk water, in the τ_{sw} time scale. We show below that this subset of water molecules, those in direct interaction with the solute, comprise, except for Xe, ~1/3 of the hydration shell; note still that, since it is unlikely to have molecules pointing two free OH groups to the solute, this affects ~1/6 of the OH groups in the hydration layer.

From Table 3, it can further be seen, however, that the HB switch frequency in the solutes' hydration shell is much lower than that for bulk and neat water at 298 K and even than for water at 283 K.

Figure 4 shows the radial dependence of the switch and reform times and frequencies around the different solutes. The switch time and frequency are longer and lower, respectively, near the solutes, following the above discussion, while the reform time and frequency are nearly unperturbed relative to bulk water (see Table 3). Hence, excluded volume water depletion strongly hinders HB acceptor switches, increasing the HB lifetimes and slowing down the orientational mobility of water. These results are consistent with previous MD studies[35,38,39] and with 2D IR spectroscopy experiments,[24] the latter suggesting that in the hydrophobic hydration shell of tetramethylurea the rate of the jumping events sharply decreases, which, in turn, strongly slows the rotation of the water molecules. The switch frequency decrease observed here, however, is not enough to induce rotational "freezing" in agreement with previous MD results.[39,44]

The switch and reform frequencies given in Table 3 permit one to dissociate the mean HB dynamics of water in two periodic events with periods given by the inverse of the respective mean frequencies. The mean (continuous) τ_{HB} can be related to the switch and reform times and frequencies by the following equation

$$\tau_{HB} = \frac{2 - \tau_{sw}f_{sw} - \tau_{rf}f_{rf}}{f_{sw} + f_{rf}} \quad (3)$$

where the 2 appears because the frequencies in Table 3 are given per water molecule rather than per OH group; HB lifetimes computed through this equation differ by less than ~0.01 ps from those given in Table 2. Further, the mean HB lifetimes between acceptor switches, τ_{HB}^{sw}, and break/reform, τ_{HB}^{rf}, events come, $\tau_{HB}^{sw} = T_{sw} - \tau_{sw}$ and $\tau_{HB}^{rf} = T_{rf} - \tau_{rf}$, where $T_{sw} = 2/f_{sw}$ and $T_{rf} = 2/f_{rf}$ are the respective switch and reform periods (see Figure 5); note that the times of switch, τ_{sw}, and reform, τ_{rf}, are, respectively, switch and reform broken HB lifetimes and because $T_{sw} \gg \tau_{sw}$ and $T_{rf} \gg \tau_{rf}$, we have $\tau_{HB}^{sw} \approx T_{sw}$ and $\tau_{HB}^{rf} \approx T_{rf}$. Thus, since $T_{sw} > T_{rf}$, τ_{HB} is largely determined by the HB break/reform dynamics (T_{rf}); longer

dx.doi.org/10.1021/jp500067a | J. Phys. Chem. B 2014, 118, 4169−4176

Table 3. HB Switch and Reform Mean Times, τ, in ps and Frequencies, f, in ps^{-1} [a]

	1st HSh[b]		bulk[c]		1st HSh		bulk		sw
	τ_{sw}	τ_{rf}	τ_{sw}	τ_{rf}	f_{sw}	f_{rf}	f_{sw}	f_{rf}	$T_{sw}^{HSh}/T_{sw}^{bulk}$
$(H_2O)_{298K}$	0.046	0.027	0.027	0.025	3.3	5.7	3.5	5.9	1.1
$(H_2O)_{283K}$	0.048	0.027	0.026	0.024	2.7	5.0	2.9	5.2	1.1
$(Xe)_{aq,297K}$	0.031	0.025	0.027	0.025	2.4	5.6	3.4	5.8	1.4
$(CH_4)_{aq,301K}$	0.031	0.025	0.027	0.025	2.6	5.8	3.6	6.0	1.4
$(C_2H_6)_{aq,300K}$	0.033	0.026	0.027	0.025	2.5	5.8	3.5	6.0	1.4
$(C_6H_6)_{aq,298K}$	0.040	0.028	0.026	0.025	2.5	5.8	3.5	5.8	1.4

[a] f is defined as the number of HBs that break and form (sw) or reform (rf) per picosecond and water molecule; sw stands for switch acceptor and rf stands for reform with the original acceptor. For pure water, a single water molecule was taken as the solute and HBs between water molecules in the self-hydration shell and the "solute" water molecule were neglected. [b] For pure water, τ_{HB} was computed for water molecules in the first and second self-hydration shells (see Methods). [c] The bulk region for neat water was defined as the region beyond the second self-hydration shell, similar to the aqueous solutions definition; HB switch/reform times and frequencies of water at 298 and 283 K for the full systems are equal to the bulk values.

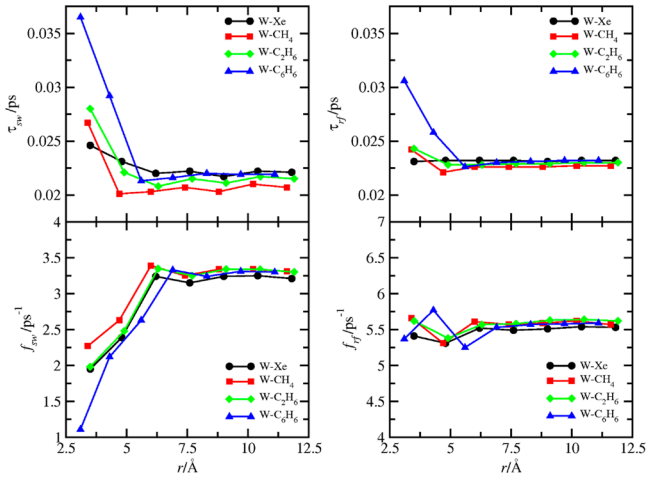

Figure 4. Radial profiles of the times and frequencies of HB switch and reform. The first two points (three for C_6H_6) encompass the first hydration shell; the first point (second for C_6H_6) corresponds to ~1/3 of the water molecules in the hydration shell. For C_6H_6, the first point is for a single water molecule with a HO−H···π HB. The nearest water molecules to the solutes take longer to switch acceptors, contributing to a faster decay of $C_2(t)$ in this time scale, t_{sw}, but molecules in the first HSh switch acceptors less often, significantly slowing down the orientational dynamics of water.

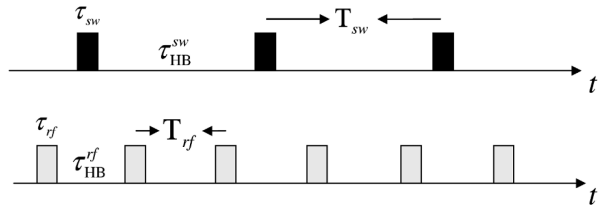

Figure 5. Scheme illustrating the mean HB break/(re)form dynamics of water. The OH groups are H-bonded during both τ_{HB}^{sw} and τ_{HB}^{rf}. The rectangles represent the mean time broken HBs take to either switch acceptors, τ_{sw}, or reform, τ_{rf}, with the original acceptor ($\tau_{sw} \neq \tau_{rf}$). Orientational relaxation occurs mostly through the HB break/form dynamics; T_{sw} and, therefore, τ_{HB}^{sw} increase significantly next to hydrophobic solutes, slowing down the orientational relaxation of water.

(intermittent) HB lifetimes, where transiently broken HBs are neglected, are given by $\tau_{HB}^{sw} = T_{sw} - \tau_{sw}$.

Now, the orientational mobility retardation in the solutes' hydration shell is determined, apart from a minor HB break/reform induced slowdown, $T_{rf}^{HSh} > T_{rf}^{bulk}$, and an acceleration associated with $\tau_{sw}^{HSh} > \tau_{sw}^{bulk}$, by the break/form dynamics, and, $T_{sw}^{HSh}/T_{sw}^{bulk} = 1.4$, similar to τ_{HSh}/τ_{bulk} for the distinct solutes (see Tables 1 and 3).[65] Notice that a longer T_{rf} (lower f_{rf}) entails a smaller contribution from librations to the loss of anisotropy,[24,31] while a larger τ_{sw} (longer broken HB lifetimes) adds to the anisotropy loss. Longer τ_{sw} values do not imply, however, a larger orientational mobility, and therefore a larger anisotropy loss, since τ_{sw} also depends on the strength of water−solute interactions. Thus, for C_6H_6, a larger τ_{sw}, relative to Xe, CH_4, and C_2H_6, is associated with the fact that a water−water broken HB is "stabilized" by a HO−H···π HB (see Figure 4); a more clear-cut example is that for the solute "water" (see Table 3), where a larger τ_{sw}, relative to the hydrophobic solutes, means a lower contribution to the relaxation of $C_2(t)$, since water molecules are H-bonded to the "solute". Note also that for neat water $T_{sw}^{HSh}/T_{sw}^{bulk} = 1.1$, indicating that the observed frequency decrease in the solutes' hydration layer is not associated with the definition of a hydration shell, always arbitrary to some extent, because of water molecules that cross the shell before reforming or switching partners; a retardation factor slightly above 1.0 is expected, since HBs with the "solute" water molecule are neglected.

Tetrahedrality and Orientational Mobility of Water. The tetrahedrality of the HB network of water was probed with recourse to the orientational order parameter,[66] q, in the rescaled form,[67] $q = 1 - (3/8)\sum_{i=1}^{3}\sum_{j=i+1}^{4}(\cos\theta_{ij} + 1/3)^2$, where θ_{ij} is the angle formed by the lines joining the O atom of a given water molecule and those of its nearest neighbors, i and j ($\leq$4); the average value of q varies between 0 (ideal gas) and 1 (perfect tetrahedral HB network). The mean tetrahedrality and the mean O distance to the four nearest water neighbors,[18] r_{O4}, in the solutes' hydration layer are given in Table 4.

We computed the tetrahedrality for every water molecule in the hydration layer and for a subset of water molecules formed by molecules whose four nearest neighbors are water molecules. Thus, if at least one of the four nearest neighbors of an O atom is a solute atom, the tetrahedrality of this water molecule is neglected. The mean number of excluded water molecules corresponds to ~1/3 of the coordination number, except for Xe (see Table 4).

Figure 6 shows that the tetrahedrality distribution for this subset of water molecules is similar to that for water at 283 K. Further, a contraction of r_{O4}, similar to that observed for water at low T[51] is found, again except for Xe. The mean O−H intermolecular distance probed here by the distance between waters' oxygen and the nearest two protons of neighbor waters,[18,51] r_{OH2}, is also smaller and the mean number of HBs is

dx.doi.org/10.1021/jp500067a | J. Phys. Chem. B 2014, 118, 4169−4176

Table 4. Mean Tetrahedral Orientational Order, q, and r_{O4} Distance for Neat Water and for the First Hydration Shell (HSh) and Bulk for the Distinct Solutes

	q 1st HSh			r_{O4} (Å) 1st HSh		
	full[a]	subset[b,c]	q bulk	full	subset	r_{O4} (Å) bulk
$(H_2O)_{298K}$			0.653			2.89
$(H_2O)_{283K}$			0.680			2.88
$(Xe)_{aq,297K}$	0.669	0.671	0.659	2.90	2.90	2.89
$(CH_4)_{aq,301K}$	0.659	0.677	0.652	2.90	2.88	2.89
$(C_2H_6)_{aq,300K}$	0.661	0.682	0.653	2.90	2.88	2.89
$(C_6H_6)_{aq,298K}$	0.647	0.671	0.655	2.90	2.88	2.89

[a]The coordination number of the s−O (s = Xe, CH_4, C_2H_6, and C_6H_6) radial distribution functions are, respectively, 21.4, 18.9, 22.3, and 29.1. [b]The mean number of water molecules excluded as tetrahedron centers in the subsets were, respectively, <1, 6.4, 8.2, and 10.0, for Xe, CH_4, C_2H_6, and C_6H_6. These water molecules are only excluded as tetrahedron centers still occupying the vertices of tetrahedrons in the computation of q; similarly, water molecules in the second hydration shell also occupy vertices of tetrahedrons at the outer edge of the first hydration layer. [c]The tetrahedrality computed here in a region, R_2, bounded by the first maximum and minimum of the s−O rdf studied in ref 18 is 0.674, 0.665, 0.669, and 0.667 for Xe, CH_4, C_2H_6, and C_6H_6, respectively; the reason for a lower q in R_2 (except for Xe) is that some water molecules in the latter region do not have four nearest water neighbors. A contraction of r_{O4}, not observed[18] in R_2, is also found in this subset, again except for Xe. Although water molecules next to Xe keep their four nearest water neighbors, the nearest pentamers are less tetrahedral than those away from Xe's surface.[18]

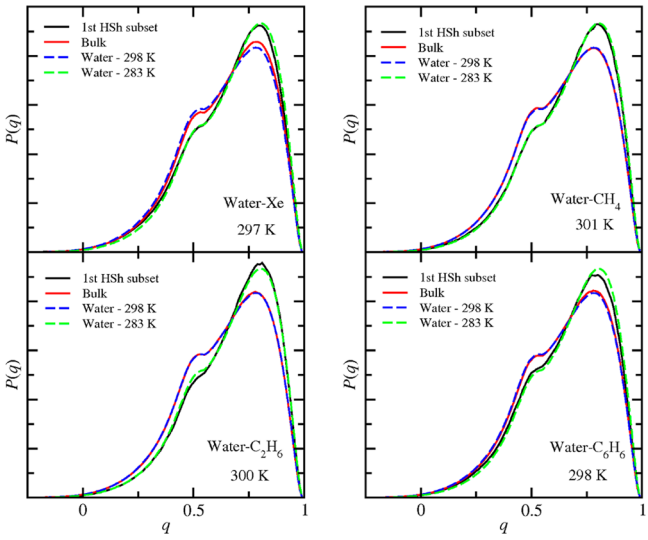

Figure 6. Tetrahedrality distribution for a subset of water molecules in the first hydration layer and bulk of the distinct solutes' aqueous solutions. The tetrahedrality of neat water at 298 and 283 K is also shown.

slightly larger (see the Supporting Information, Table S1 and Figure S3); distributions of r_{O4} and r_{OH2} are given in the Supporting Information (Figures S4 and S5). Thus, large structural resemblances between this water ensemble and water at 283 K can be observed. This structural transformation cannot, however, be recognized when the full hydration layer is probed, despite the excluded waters occupy the vertices of the enhanced tetrahedrality water pentamers (see Table 4).

We now turn attention to the effect of this structural enhancement on the HB dynamics of water. We calculated the mean HB lifetime and the switch and reform times and frequencies for this water subset. It should be noted, nonetheless, that excluded volume and water structuring effects cannot be fully disentangled. Thus, while water molecules in this ensemble have four nearest water neighbors, those nearest to the solute still experience a lower number of waters accessible to switch HB partners; interestingly, the greater strength of HBs near hydrophobic groups in a protein has recently been shown to be correlated with the depletion of water.[68] The mean distance of the fifth[69] nearest water neighbor, involved in the HB switch mechanism,[39,56] slightly decreases relative to the mean value in the first hydration shell, but it remains larger than for bulk water (see the Supporting Information, Table S2). A decrease of the time of switch, below τ_{sw} for bulk water, is observed (see the Supporting Information, Table S2); for instance, for C_2H_6, τ_{sw} is 0.022 ps compared to 0.033 and 0.027 ps for the hydration shell and bulk water, respectively. The switch frequency increases, from 2.5 to 3.0 ps^{-1}, although below the mean frequency for bulk water, 3.5 ps^{-1}, while the reform frequency and the mean (continuous) HB lifetime are similar to those for bulk water. Thus, in a more tetrahedral environment (and same T), HB donors switch acceptors less frequently but faster than in less tetrahedral (bulk) water, although the reduction of f_{sw} should be still largely a water depletion effect; a HB dynamics retardation factor, $T_{sw}^{HSh\text{-}sub}/T_{sw}^{bulk} = 1.2$, is found for this subset of water molecules. The fact that both f_{sw} and f_{rf} significantly decrease for neat water at lower T, unlike for this water ensemble (see Table 2 and Table S2 in the Supporting Information), despite of the structural similarities, further indicates that the structure of water should play a minor role on the orientational slowdown of water. This result is also in accord with previous MD studies which concluded that stronger HBs alone could not account for the HB dynamics and orientational slowdown of water next to different hydrophobic groups,[35,38] imputing the latter to excluded volume effects.[39] Similar conclusions concerning the small effect of water structuring on the orientational dynamics of water at room temperature have also been recently reported through a different approach.[43] Thus, although a structural enhancement takes place near hydrophobic solutes, this appears to play a minor part adding to the orientational slowdown of water mostly by reducing (relative to the bulk) τ_{sw} and possibly, to some extent, f_{sw}.

SUMMARY

The structure, HB dynamics, and orientational mobility of water near small hydrophobic solutes at room temperature was studied through molecular dynamics. Our results show that the orientational slowdown observed near small apolar solutes is mostly induced by a decrease of the HB break/form frequency caused by excluded volume effects. HB (continuous) lifetimes are, in turn, determined by the HB break/reform dynamics, not significantly perturbed near the hydrophobic solutes, thus explaining a lower retardation factor compared with that observed for the orientational dynamics. Further, volume exclusion leads to longer switch times (i.e., broken HB lifetimes between acceptor switches) possibly slightly accelerating the orientational relaxation of ∼1/3 of the water molecules on the hydration layer on this time scale. Even though a subset (∼2/3) of water molecules in the hydration shell of small hydrophobic solutes have a structure similar to that observed for neat water

dx.doi.org/10.1021/jp500067a | J. Phys. Chem. B 2014, 118, 4169−4176

at ∼10 °C, this structural enhancement appears to make only a minor contribution to this slowdown. Thus, despite that excluded volume and water structuring effects cannot be fully disentangled, this structural contribution to the orientational slowdown seems to result mostly from a slight decrease of the broken HB lifetimes near the solutes.

■ ASSOCIATED CONTENT

Supporting Information

Methodological details along with additional tables and figures supporting our conclusions are provided. This material is available free of charge via the Internet at http://pubs.acs.org.

■ AUTHOR INFORMATION

Corresponding Author

*E-mail: ngalamba@cii.fc.ul.pt.

Notes

The authors declare no competing financial interest.

■ ACKNOWLEDGMENTS

The author gratefully acknowledges financial support from Fundação para a Ciência e a Tecnologia from Portugal through the project PTDC/QUI-QUI/113376/2009.

■ REFERENCES

(1) Ball, P. Water as an Active Constituent in Cell Biology. *Chem. Rev.* **2008**, *108*, 74−108.

(2) Chandler, D. Interfaces and the Driving Force of Hydrophobic Assembly. *Nature* **2005**, *437*, 640−647.

(3) Kauzmann, W. Some Factors in the Interpretation of Protein Denaturation. *Adv. Protein Chem.* **1959**, *14*, 1−63.

(4) Privalov, P. L.; Gill, S. J. Stability of Protein-Structure and Hydrophobic Interaction. *Adv. Protein Chem.* **1988**, *39*, 191−234.

(5) Frank, H. S.; Evans, M. W. Free Volume and Entropy in Condensed Systems 0.3. Entropy in Binary Liquid Mixures - Partial Molal Entropy in Dilute Solutions - Structure and Thermodynamics in Aqueous Electrolytes. *J. Chem. Phys.* **1945**, *13*, 507−532.

(6) Southall, N. T.; Dill, K. A.; Haymet, A. D. J. A View of the Hydrophobic Effect. *J. Phys. Chem. B* **2002**, *106*, 521−533.

(7) Buchanan, P.; Aldiwan, N.; Soper, A. K.; Creek, J. L.; Koh, C. A. Decreased Structure on Dissolving Methane in Water. *Chem. Phys. Lett.* **2005**, *415*, 89−93.

(8) Soper, A. K.; Finney, J. L. Hydration of Methanol in Aqueous-Solution. *Phys. Rev. Lett.* **1993**, *71*, 4346−4349.

(9) Turner, J.; Soper, A. K. The Effect of Apolar Solutes on Water Structure: Alcohols and Tetraalkylammonium Ions. *J. Chem. Phys.* **1994**, *101*, 6116−6125.

(10) Ashbaugh, H. S.; Pratt, L. R. Colloquium: Scaled Particle Theory and the Length Scales of Hydrophobicity. *Rev. Mod. Phys.* **2006**, *78*, 159−178.

(11) Ashbaugh, H. S.; Truskett, T. M.; Debenedetti, P. G. A Simple Molecular Thermodynamic Theory of Hydrophobic Hydration. *J. Chem. Phys.* **2002**, *116*, 2907−2921.

(12) Garde, S.; Hummer, G.; Garcia, A. E.; Paulaitis, M. E.; Pratt, L. R. Origin of Entropy Convergence in Hydrophobic Hydration and Protein Folding. *Phys. Rev. Lett.* **1996**, *77*, 4966−4968.

(13) Hummer, G.; Garde, S.; Garcia, A. E.; Pohorille, A.; Pratt, L. R. An Information Theory Model of Hydrophobic Interactions. *Proc. Natl. Acad. Sci. U.S.A.* **1996**, *93*, 8951−8955.

(14) Lee, B.; Graziano, G. A Two-State Model of Hydrophobic Hydration That Produces Compensating Enthalpy and Entropy Changes. *J. Am. Chem. Soc.* **1996**, *118*, 5163−5168.

(15) Lum, K.; Chandler, D.; Weeks, J. D. Hydrophobicity at Small and Large Length Scales. *J. Phys. Chem. B* **1999**, *103*, 4570−4577.

(16) Widom, B.; Bhimalapuram, P.; Koga, K. The Hydrophobic Effect. *Phys. Chem. Chem. Phys.* **2003**, *5*, 3085−3093.

(17) Stillinger, F. H. Structure in Aqueous Solutions of Nonpolar Solutes from the Standpoint of Scaled-Particle Theory. *J. Solution Chem.* **1973**, *2*, 141−158.

(18) Galamba, N. Water's Structure around Hydrophobic Solutes and the Iceberg Model. *J. Phys. Chem. B* **2013**, *117*, 2153−2159.

(19) Song, B.; Molinero, V. Thermodynamic and Structural Signatures of Water-Driven Methane-Methane Attraction in Coarse-Grained Mw Water. *J. Chem. Phys.* **2013**, *139*, 054511.

(20) Jana, B.; Pal, S.; Bagchi, B. Enhanced Tetrahedral Ordering of Water Molecules in Minor Grooves of DNA: Relative Role of DNA Rigidity, Nanoconfinement, and Surface Specific Interactions. *J. Phys. Chem. B* **2010**, *114*, 3633−3638.

(21) Davis, J. G.; Gierszal, K. P.; Wang, P.; Ben-Amotz, D. Water Structural Transformation at Molecular Hydrophobic Interfaces. *Nature* **2012**, *491*, 582−585.

(22) Nakahara, M.; Wakai, C.; Yoshimoto, Y.; Matubayasi, N. Dynamics of Hydrophobic Hydration of Benzene. *J. Phys. Chem.* **1996**, *100*, 1345−1349.

(23) Nakahara, M.; Yoshimoto, Y. Hydrophobic Slowdown and Hydrophilic Speedup of Water Rotation in Supercooled Aqueous Solutions of Benzene and Phenol. *J. Phys. Chem.* **1995**, *99*, 10698−10700.

(24) Bakulin, A. A.; Liang, C.; Jansen, T. L.; Wiersma, D. A.; Bakker, H. J.; Pshenichnikov, M. S. Hydrophobic Solvation: A 2d Ir Spectroscopic Inquest. *Acc. Chem. Res.* **2009**, *42*, 1229−1238.

(25) Bakulin, A. A.; Pshenichnikov, M. S.; Bakker, H. J.; Petersen, C. Hydrophobic Molecules Slow Down the Hydrogen-Bond Dynamics of Water. *J. Phys. Chem. A* **2011**, *115*, 1821−1829.

(26) Haselmeier, R.; Holz, M.; Marbach, W.; Weingaertner, H. Water Dynamics near a Dissolved Noble Gas. First Direct Experimental Evidence for a Retardation Effect. *J. Phys. Chem.* **1995**, *99*, 2243−2246.

(27) Ishihara, Y.; Okouchi, S.; Uedaira, H. Dynamics of Hydration of Alcohols and Diols in Aqueous Solutions. *J. Chem. Soc., Faraday Trans.* **1997**, *93*, 3337−3342.

(28) Kaatze, U.; Gerke, H.; Pottel, R. Dielectric Relaxation in Aqueous Solutions of Urea and Some of Its Derivatives. *J. Phys. Chem.* **1986**, *90*, 5464−5469.

(29) Okouchi, S.; Moto, T.; Ishihara, Y.; Numajiri, H.; Uedaira, H. Hydration of Amines, Diamines, Polyamines and Amides Studied by Nmr. *J. Chem. Soc., Faraday Trans.* **1996**, *92*, 1853−1857.

(30) Qvist, J.; Halle, B. Thermal Signature of Hydrophobic Hydration Dynamics. *J. Am. Chem. Soc.* **2008**, *130*, 10345−10353.

(31) Rezus, Y. L. A.; Bakker, H. J. Observation of Immobilized Water Molecules around Hydrophobic Groups. *Phys. Rev. Lett.* **2007**, *99*, 148301.

(32) Shimizu, A.; Fumino, K.; Yukiyasu, K.; Taniguchi, Y. Nmr Studies on Dynamic Behavior of Water Molecule in Aqueous Denaturant Solutions at 25 Degrees C: Effects of Guanidine Hydrochloride, Urea and Alkylated Ureas. *J. Mol. Liq.* **2000**, *85*, 269−278.

(33) Wachter, W.; Buchner, R.; Hefter, G. Hydration of Tetraphenylphosphonium and Tetraphenylborate Ions by Dielectric Relaxation Spectroscopy. *J. Phys. Chem. B* **2006**, *110*, 5147−5154.

(34) Yoshida, K.; Ibuki, K.; Ueno, M. Pressure and Temperature Effects on H-2 Spin-Lattice Relaxation Times and H-1 Chemical Shifts in Tert-Butyl Alcohol- and Urea-D2o Solutions. *J. Chem. Phys.* **1998**, *108*, 1360−1367.

(35) Xu, H. F.; Berne, B. J. Hydrogen-Bond Kinetics in the Solvation Shell of a Polypeptide. *J. Phys. Chem. B* **2001**, *105*, 11929−11932.

(36) Linse, P. Molecular Dynamics Simulation of a Dilute Aqueous Solution of Benzene. *J. Am. Chem. Soc.* **1990**, *112*, 1744−1750.

(37) Geiger, A.; Rahman, A.; Stillinger, F. H. Molecular Dynamics Study of the Hydration of Lennard-Jones Solutes. *J. Chem. Phys.* **1979**, *70*, 263−276.

(38) Rossky, P. J.; Karplus, M. Solvation. A Molecular Dynamics Study of a Dipeptide in Water. *J. Am. Chem. Soc.* **1979**, *101*, 1913−1937.

(39) Laage, D.; Stirnemann, G.; Hynes, J. T. Why Water Reorientation Slows without Iceberg Formation around Hydrophobic Solutes. *J. Phys. Chem. B* **2009**, *113*, 2428−2435.
(40) Rossato, L.; Rossetto, F.; Silvestrelli, P. L. Aqueous Solvation of Methane from First Principles. *J. Phys. Chem. B* **2012**, *116*, 4552−4560.
(41) Zichi, D. A.; Rossky, P. J. Solvent Molecular-Dynamics in Regions of Hydrophobic Hydration. *J. Chem. Phys.* **1986**, *84*, 2814−2822.
(42) Silvestrelli, P. L. Are There Immobilized Water Molecules around Hydrophobic Groups? Aqueous Solvation of Methanol from First Principles. *J. Phys. Chem. B* **2009**, *113*, 10728−10731.
(43) Duboue-Dijon, E.; Fogarty, A. C.; Laage, D. Temperature Dependence of Hydrophobic Hydration Dynamics: From Retardation to Acceleration. *J. Phys. Chem. B* **2014**, *118*, 1574−1583.
(44) Stirnemann, G.; Hynes, J. T.; Laage, D. Water Hydrogen Bond Dynamics in Aqueous Solutions of Amphiphiles. *J. Phys. Chem. B* **2010**, *114*, 3052−3059.
(45) Titantah, J. T.; Karttunen, M. Long-Time Correlations and Hydrophobe-Modified Hydrogen-Bonding Dynamics in Hydrophobic Hydration. *J. Am. Chem. Soc.* **2012**, *134*, 9362−9368.
(46) Ren, P. Y.; Ponder, J. W. Consistent Treatment of Inter- and Intramolecular Polarization in Molecular Mechanics Calculations. *J. Comput. Chem.* **2002**, *23*, 1497−1506.
(47) Ren, P. Y.; Ponder, J. W. Polarizable Atomic Multipole Water Model for Molecular Mechanics Simulation. *J. Phys. Chem. B* **2003**, *107*, 5933−5947.
(48) Ponder, J. W. *Tinker: Software Tools for Molecular Design 5.1*; Washington University School of Medicine: Saint Louis, MO, 2010.
(49) Berendsen, H. J. C.; Postma, J. P. M.; Vangunsteren, W. F.; Dinola, A.; Haak, J. R. Molecular Dynamics with Coupling to an External Bath. *J. Chem. Phys.* **1984**, *81*, 3684−3690.
(50) Starr, F. W.; Nielsen, J. K.; Stanley, H. E. Fast and Slow Dynamics of Hydrogen Bonds in Liquid Water. *Phys. Rev. Lett.* **1999**, *82*, 2294−2297.
(51) Galamba, N. On the Effects of Temperature, Pressure and Dissolved Salts on the Hydrogen-Bond Network of Water. *J. Phys. Chem. B* **2013**, *117*, 589−601.
(52) Martiniano, H. F. M. C.; Galamba, N. Insights on Hydrogen-Bond Lifetimes in Liquid and Supercooled Water. *J. Phys. Chem. B* **2013**, *117*, 16188−16195.
(53) Luzar, A. Resolving the Hydrogen Bond Dynamics Conundrum. *J. Chem. Phys.* **2000**, *113*, 10663−10675.
(54) Paesani, F.; Voth, G. A. The Properties of Water: Insights from Quantum Simulations. *J. Phys. Chem. B* **2009**, *113*, 5702−5719.
(55) Giguére, P. A. The Bifurcated Hydrogen-Bond Model of Water and Amorphous Ice. *J. Chem. Phys.* **1987**, *87*, 4835−4839.
(56) Laage, D.; Hynes, J. T. A Molecular Jump Mechanism of Water Reorientation. *Science* **2006**, *311*, 832−835.
(57) Luzar, A. Water Hydrogen-Bond Dynamics Close to Hydrophobic and Hydrophilic Groups. *Faraday Discuss.* **1996**, *103*, 29−40.
(58) Henchman, R. H.; Cockram, S. J. Water's Non-Tetrahedral Side. *Faraday Discuss.* **2013**, *167*, 529−550.
(59) Eaves, J. D.; Loparo, J. J.; Fecko, C. J.; Roberts, S. T.; Tokmakoff, A.; Geissler, P. L. Hydrogen Bonds in Liquid Water Are Broken Only Fleetingly. *Proc. Natl. Acad. Sci. U.S.A.* **2005**, *102*, 13019−13022.
(60) Allesch, M.; Schwegler, E.; Galli, G. Structure of Hydrophobic Hydration of Benzene and Hexafluorobenzene from First Principles. *J. Phys. Chem. B* **2007**, *111*, 1081−1089.
(61) Atwood, J. L.; Hamada, F.; Robinson, K. D.; Orr, G. W.; Vincent, R. L. X-Ray Diffraction Evidence for Aromatic Pi Hydrogen-Bonding to Water. *Nature* **1991**, *349*, 683−684.
(62) Mateus, M. P. S.; Galamba, N.; Cabral, B. J. C. Structure and Electronic Properties of a Benzene-Water Solution. *J. Chem. Phys.* **2012**, *136*.
(63) Raschke, T. M.; Levitt, M. Detailed Hydration Maps of Benzene and Cyclohexane Reveal Distinct Water Structures. *J. Phys. Chem. B* **2004**, *108*, 13492−13500.
(64) Schravendijk, P.; van der Vegt, N. F. A. From Hydrophobic to Hydrophilic Solvation: An Application to Hydration of Benzene. *J. Chem. Theory Comput.* **2005**, *1*, 643−652.
(65) The dependence of water HB lifetimes on the HB definition was recently considered in ref 52; it was shown that, when transient HBs and transiently broken HBs are neglected, HB definition (geometric and geometric/energetic) independent lifetimes are obtained. Here, since the break/reform HB dynamics (transiently broken HBs) is not significantly perturbed near the solutes, we believe that transient HBs (not excluded) should not significantly change the HB switch period ratios given in the last column of Table 3.
(66) Chau, P. L.; Hardwick, A. J. A New Order Parameter for Tetrahedral Configurations. *Mol. Phys.* **1998**, *93*, 511−518.
(67) Errington, J. R.; Debenedetti, P. G. Relationship between Structural Order and the Anomalies of Liquid Water. *Nature* **2001**, *409*, 318−321.
(68) Matysiak, S.; Debenedetti, P. G.; Rossky, P. J. Dissecting the Energetics of Hydrophobic Hydration of Polypetides. *J. Phys. Chem. B* **2011**, *115*, 14859−14865.
(69) Sciortino, F.; Geiger, A.; Stanley, H. E. Effect of Defects on Molecular Mobility in Liquid Water. *Nature* **1991**, *354*, 218−221.